11th International Symposium on Magnetic Bearings
August 26-29, Nara, Japan

EFFECT OF LONG CABLES ON AMB SYSTEMS

Nicholas Elder
TRAX, LLC., Forest, VA 24551 USA
nelder@gmail.com

Eric Maslen
Dept. of Mech. and Aero. Engineering, University of Virginia, Charlottesville, VA 22904 USA
ehm7s@virginia.edu

ABSTRACT

The electrical properties of long cable bundles are modeled and measured and the potential impact on the performance of active magnetic bearing systems is investigated. A model able to accurately predict the electrical impedance of twisted pair, both shielded and unshielded, is developed and validated. The model is then extended to explore coupling between such cable sets and the resulting noise that can be induced by switching amplifiers on sensor cabling. Specific recommendations are provided for improving amplifier stability with long cables and for minimizing noise ingress to sensor cables adjacent to noisy coil drive cables.

INTRODUCTION

Many potential applications of active magnetic bearings favor large separations between the machinery and the drive/sensing electronics. This separation may be dictated by environmental considerations or a broader interest in consolidating electronics and control systems into a centralized facility. Separations as long as 1 km are envisioned in certain applications. This large separation motivates an interest in understanding the potential impact of these long cables on the performance of the AMB system and raises the question of whether it is even practical to implement such large separation.

The present study investigates the following questions: 1) How can the cable be modeled for the purpose of studying stability of the amplifier/cable/magnet coil combination? 2) How can we model the coupling of amplifier noise to sensor signal wires? and 3) How should sensor signals best be transmitted and received in order to minimize noise?

CABLE MODEL

Cable bundles typically include a combination of unshielded twisted pairs (UTP) and shielded twisted pairs (STP). A suitable model needs to consider both potential kinds of cable and their interactions. We start by examining UTP, then proceed to STP and finally develop a model for interaction between the two.

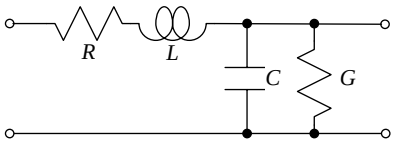

Figure 1: Basic model of an element of an unshielded twisted pair, from [3]. Leakage conductance, G, is generally ignored.

Unshielded Twisted Pairs

Models of cable in the literature fall roughly into two categories: finite element and continuum. The primary finite element model of twisted pair [3] is quite simple, depicted in Figure 1. Notice that this model appears not to be symmetric in that only the upper path contains resistive or inductive elements. In fact, if the twisted pair is driven symmetrically, this model presents the corresponding cable impedance and, given its simplicity, provides a compact and efficient form to model twisted pair. However, if the twisted pair is not driven symmetrically - as in the case of coil drive in an AMB (the two conductors are alternately connected to the supply bus or to ground) - then the model cannot properly describe the resulting cable dynamics, particularly the instantaneous potential distribution along each cable relative to ground.

A further shortcoming relates to the fact that the effective element resistance and inductance is independent of frequency. In reality, the effective resistance of the cable increases with increasing frequency due to skin effects in the cable. At the same time and due to the same effect, the inductance of the cable decreases with increas-

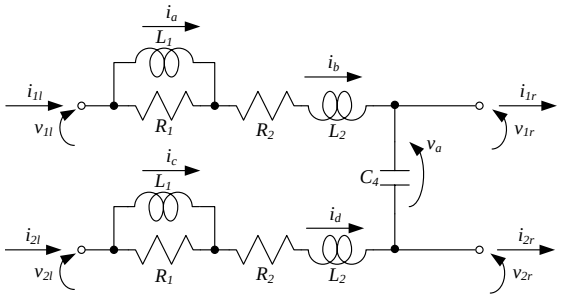

Figure 2: Finite element of the unshielded twisted pair model with skin effect approximation.

ing frequency. Neither of these behaviors is captured in the available finite element models in the open literature: more commonly, these models are tuned to a particular signal transmission frequency by adjusting the resistance and inductance to account for skin effect [2, 8]. Continuum cable models in the literature [1, 6] do account for these effects, but are not tractable for normal engineering purposes.

The element schematic detailed in Figure 2 largely repairs these problems. By using a symmetric structure, it permits asymmetric drive of the cable. The added resistor/inductor pair (R_1, L_1) tend to increase the element resistance at high frequency (L_1 blocks) while reducing the inductance. The details of constructing a full electrical model from this element are provided in [4].

Choosing the parameters of this more complex model is not difficult. Twisted pair cable comes with a characterization of resistance, inductance, and capacitance per unit length: these numbers compare favorably to calculations available in the literature [5].

These numbers are used to obtain R_2, L_2, and C_4 [4]. The parameters R_1 and L_l can then be tuned to match published predictions of frequency dependent resistance [2, 8] at a particular frequency (the finite order of this skin effect model precludes matching at all frequencies). In the work discussed here, we matched the resistance at the first cable mode (about 280 kHz).

The model was experimentally validated by examining both its frequency response and its transient response in comparison to the same measurements for a physical cable with a length of 150 m. Figure 3 compares the experimental data to that generated by both the conventional model of Figure 1 and by the model proposed here. What is most significant is that the relatively simple correction provided by the new model (just two added parameters) produces a nearly perfect variation in modal damping across the five modes measured. The improvement over the conventional model is immediately evident.

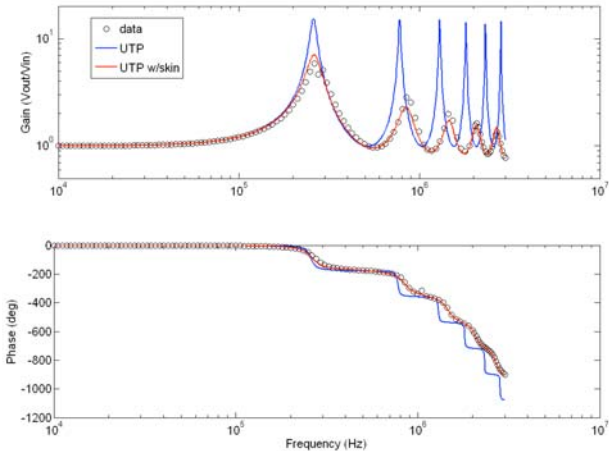

Figure 3: Experimental and simulated transfer function of 150 m length of unshielded twisted pair cable.

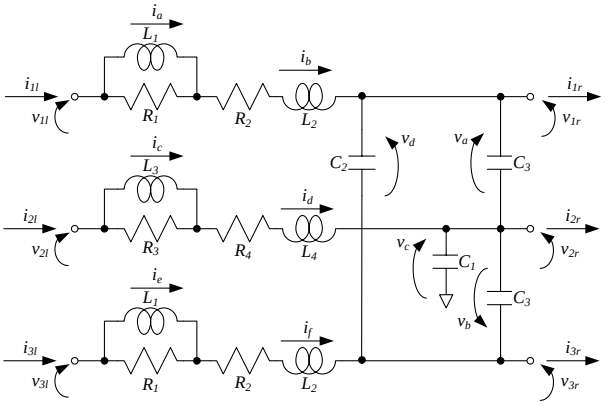

Figure 4: Finite element of the shielded twisted pair model with skin effect approximation. The *center* line is considered to be the shield.

Shielded Twisted Pair

Most applications of twisted pair to AMB systems use a shield (STP). The predominant model of STP in the literature extends the model of Figure 1 by tying its "primary" conductor to a resistive shield by distributed capacitance. The principle shortcoming to this model is that, because the shield has no inductance, potential changes applied to one end of the shield propagate to the other end instantaneously. A very simple experiment with a sufficiently long cable will confirm that the shield exhibits propagation delay just as do the conductors of the twisted pair. Hence, we adapted the model of Figure 2 to include a shield by introducing a third conductor similar to the other two with capacitive coupling to each of the other two. The resulting element model is depicted in Figure 4.

This model was also validated experimentally by measuring the transient and frequency response of a test (152 m long) cable and comparing the results to those obtained

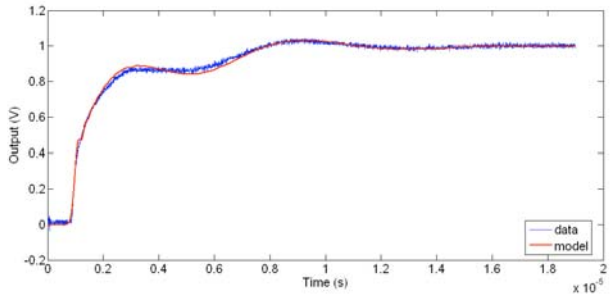

Figure 5: Transient (step) response of the far end of shielded twisted pair cable model to a step applied to the near end. Comparison to experimental measurement: cable length is 152 m.

by simulation of this model. Figure 5 shows a typical result, illustrating the fidelity of the model. Note, in particular, the delay of approximately 0.8 microseconds at the beginning of the figure. The input signal rose at $t = 0$. This delay results from the specific modal structure of the cable model and was not introduced artificially (the model contains *only* capacitors, resistors, and inductors).

Coupled Model

One of the primary goals of the project was to model coupling of coil drive cable switching noise to adjacent sensor signal cables. As such, the model must be extended to consider electrical coupling between adjacent cables. Arguably, the only strong coupling mechanism is capacitive: the twisted structure of each bundle suggests that the net magnetic field should be nearly zero adjacent to the bundle, but because the drive cable twisted pair is not driven symmetrically, the cable can be expected to generate a relatively strong net electrical field. Hence, most cable-cable coupling models in the literature are purely capacitive [7].

The model indicated in Figure 6 indicates a shielded twisted pair coupled capacitively to an unshielded twisted pair. The structure of the model is such that it can be adjusted without structural change to also model coupling between two shielded cables as long as the two shields are terminated in the same way.

Although the model is complicated and contains numerous parameters, all except the cable-cable coupling capacitance (C_5 in Figure 6) can be computed from known geometric and physical properties of the cable. Estimation of the coupling capacitance is more difficult and probably varies along the length of the cable, among other things. Consequently, some tuning of this parameter will typically be needed, or it can be used for a parametric study to establish the likely range of coupling.

Generally, as might be expected, the fidelity of the models degrades as they become more complex. First, measurement of the transfer function from the primary

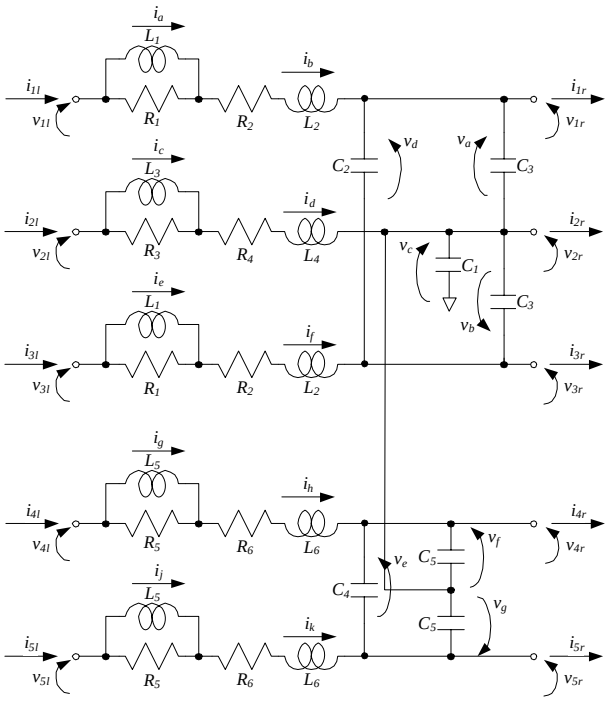

Figure 6: Element model of a coupled STP–UTP wire bundle.

conductors of the STP to its shield showed problems. Referring to Figure 7, it is evident that the model works well out to about 100 kHz (where the first coupled bundle mode arises) and then degrades rapidly after that.

One possible explanation for this problem is that, if the cable is driven single sided (one conductor is grounded at source) then current leakage to the shield is asymmetric. If so, then it is no longer true that the twisted pair ensures no magnetic field because the currents in the two conductors are not matched. Consequently, it may be necessary to consider mutual inductance between the shield and each of the individual conductors of the twisted pair: the model does not consider this effect. Of course, other effects may also be at play in degrading this model.

Since the coupled model is dependent on the fidelity of the STP coupling from signal conductors to shield, it will come as no surprise that the quality of the model of overall coupling from STP signal conductor to UTP signal conductor is relatively poor. Figure 8 compares model prediction to experimental measurement, which is relatively poor.

Model Assessment

The relatively high fidelity of the UTP and STP models, by themselves, suggests that they can accurately and quantitatively represent the added dynamics seen by a power amplifier or a sensor signal transmission scheme. Hence, the models were used for these assessments without hesitation. On the other hand, for assessing coupling

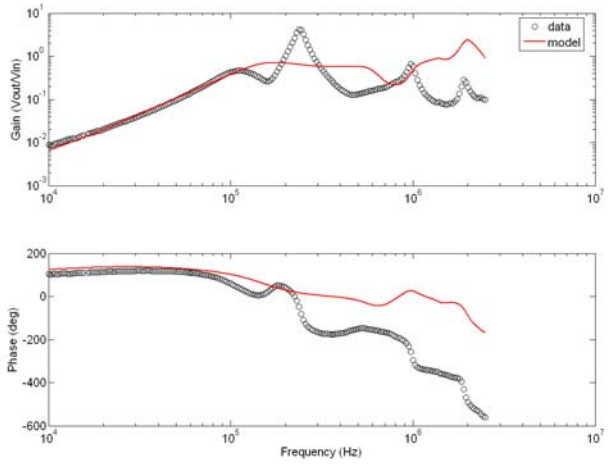

Figure 7: Transfer function from near end STP signal lead input to far end shield potential. Cable length is 152 m.

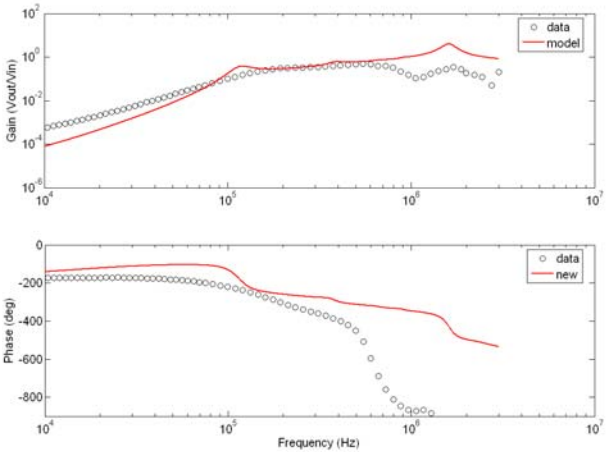

Figure 8: Coupling from near end STP conductor (driven single-sided) to near end UTP conductor. Cable length is 152 m. Comparison is poor.

of amplifier switching noise to sensor cables, the model is qualitative at best. However, it is likely that the impedance from the cable drive shield to the STP conductors is reasonably realistic. Hence, loading by noise management circuitry in the sensor transmit/receive system can be expected to be properly reflected in relative effect on transmitted noise. With this in mind, we relied on the coupled model to assess the impact of sensor cable noise management approaches, even though we recognized that the estimates of noise level could not be relied upon to be quantitative.

AMB SYSTEM ISSUES

One concern at the outset of this project was that long cables would affect system stability at the baseline model level. However, a cable with length of 150 m has its first mode at about 280 kHz: well beyond the dynamic range

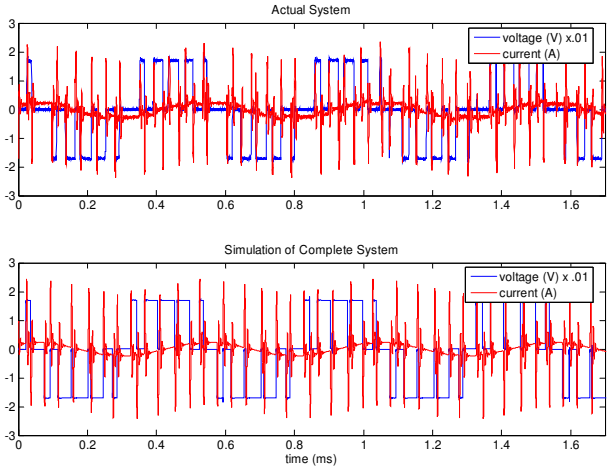

Figure 9: Comparison of simulated and measured amplifier switching.

of normal AMB system models. The first mode will vary inversely with cable length so a 1 km long cable could be expected to exhibit significant dynamics at 28 kHz, but this is still beyond the range important to AMB system models. However, both numbers imply potential effects on power amplifier stability and noise levels in received sensor signals, especially if sharp edges need to be detected. These considerations lead to a focus on amplifier dynamics and sensor noise.

Amplifier loading

To test the overall amplifier/cable/load model, we used a commercial three-state switching amplifier to drive a test inductance of roughly 20 mH connected by a 150 m length of STP. Our simulation modeled the details of the three-state drive including the H-bridge, drive logic, and analog filtering. The load was corrected for internal capacitance and eddy current effects in the massive iron structure to match the measured (local) impedance seen at the cable ends.

Figure 9 shows the fidelity of the resulting simulation. What is immediately apparent is that the simulation is remarkably good and captures the amplitude of the switching noise - both voltage and current - surprisingly well. More importantly, the simulation shows very large current spikes at each switch event. These spikes arise because the cable has a lot of capacitance while the amplifer has essentially zero output inductance.

Figure 10 shows details of a single switching pulse, indicating the very high fidelity of the model as well as reinforcing the significance of the inrush current to the cable set. These current spikes, commonly observed in AMB current sensors, are often assumed to be an artifact of poor isolation or signal grounding. These results demonstrate that they represent actual cable currents.

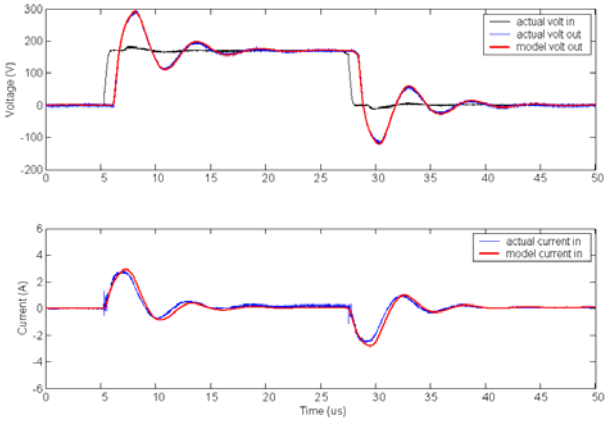

Figure 10: Detail of the amplifier switching transient. The upper plot superimposes modeled and measured *load* voltage on the cable input voltage (measured at the output of the power amplifier). Note the cable delay. The lower plot shows modeled and measured cable input current, at the drive end of the cable. Voltage measurements are differential between the two conductors of the STP.

The fact that the total load presented to the power amplifier by the cable/magnet combination can be significantly capacitive is important. Most discussions of AMB power amplifiers assume a nearly purely inductive load and this permits amplifier control algorithms specifically tailored to this kind of load. When the load is strongly capacitive, these methods may work poorly or may actually exhibit instability.

Our experimental experience supported this concern: the amplifier used in these tests was unstable for certain grounding configurations when driving the 152 m test cable bundle, exhibiting a strong limit cycle behavior triggered when the derivative of the drive signal exceeded a specific level. Figure 11 illustrates the resulting current waveforms: a large current offset of -3 A (the reference has zero offset) and some strange switching decisions (the amplifier often switches "normally" even though the error between target and actual current is very large: see, for example, the section between 2.6 msec and 4.1 msec.) The stability threshold was well below the normal slew rate limit of the amplifier/load combination: see Figure 12.

Although our simulation was unable to reproduce this instability, it is likely that cable-to-shield capacitance was the cause. The amplifier did not exhibit any evidence of stability problems when driving the load through a short (3 m) cable.

One simple palliative to this problem, not explored in our experimental work, is to simply introduce small inductors in series with each conductor of the twisted pair directly at the output of the power amplifier. By choosing these inductors to be roughly 5% of the nominal AMB coil inductance, the effect on AMB dynamic performance is minimal but the problem of current in-rush at the switching event should be substantially reduced. We believe that this would have solved the amplifier stability problem and substantially reduced the cable-borne switching noise associated with cable capacitance.

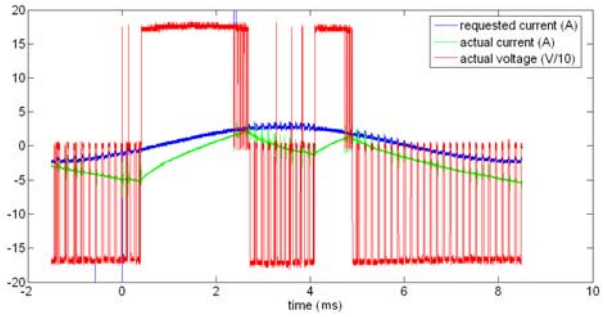

Figure 11: Example of amplifier instability: 152 m STP cable with shield grounded at one end. Requested current is ± 2.5A at 100 Hz.

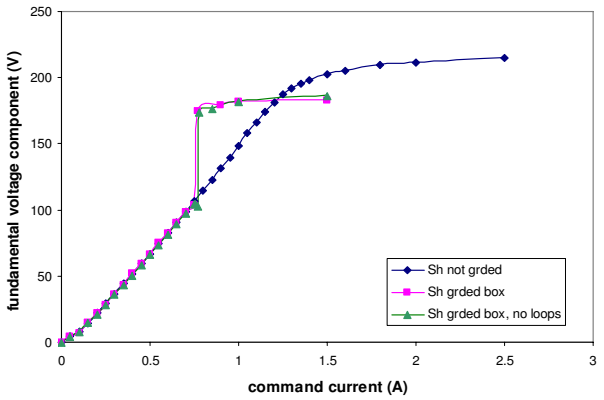

Figure 12: Output signal fundamental *vs* command signal amplitude, showing jump to limit cycle. Command frequency is 400 Hz. Power supply is 170 VDC leading to 220 volt maximum output voltage fundamental. Inductance is 52 mH so theoretical slew rate limit at 400 Hz is 1.3 A.

Sensor cable noise management

Coupling of amplifier switching noise to the sensor cable was very strong in this system, even if both cables were shielded. Initially, we assumed that this problem could be mostly eliminated by using a carefully constructed differential transmit/receive system, as illustrated in Figure 13. Such a system, if properly constructed, ensures that the source and sink impedances for the two twisted pair conductors are identical. The result is that noise infiltration to the two conductors is also essentially identical. At the same time, by driving the cable pair differentially, the signal is equal and opposite. Consequently, the cable poten-

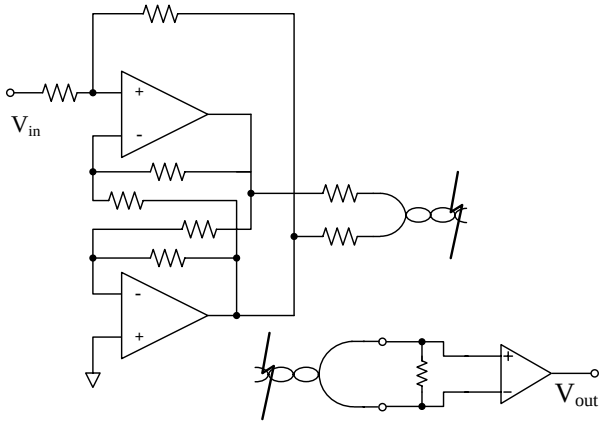

Figure 13: Differential transmit/receive circuit with a twisted pair cable.

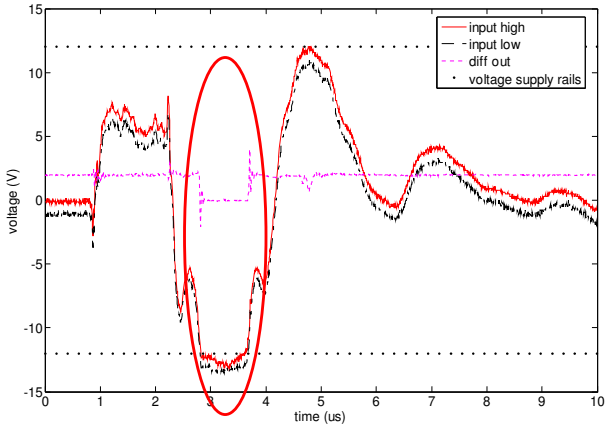

Figure 14: Common mode noise saturated the differential amplifier in testing.

tials at the receive ends should be

$$v_1 = \alpha v_s + \beta\eta \quad (1a)$$

$$v_2 = -\alpha v_s + \beta\eta \quad (1b)$$

in which v_1 and v_2 are the two cable potentials at the receive end, v_s is the signal being transmitted, η is the effective noise source, and α and β are attenuations of the two signals. Effectively, this arrangement ensures that noise is completely *common mode* while signal is completely *differential mode*. When such a pair of signals is received with a differential receiver, the output signal is

$$\begin{aligned} v_{out} &= v_1 - v_2 + \frac{1}{\mathrm{CMRR}}(v_1 + v_2) \\ &= 2\alpha v_s + \frac{2\beta}{\mathrm{CMRR}}\eta \end{aligned} \quad (2)$$

where CMRR is the differential amplifier's common mode rejection ratio: usually on the order of 70 dB or more for a high quality differential amplifier. This means that the differential scheme can reduce the noise amplitude by a factor of more than 1000 relative to what can be accomplished by a single sided transmit/receive arrangement (where one conductor is ground reference). Further, it means that it is not necessary to introduce a low pass filter to reject noise: a problem if the sensor signal has significant spectral overlap with the noise as in the case of a rotor angle reference pulse ("key phasor") signal.

However, experimental noise measurements did not support this large improvement. We discovered that the noise levels on the sensor cable were large enough that they were periodically saturating the inputs of the differential receiver. When both inputs saturate, the output goes to zero and this produces "noise" on the output of the receiver whose amplitude seems to depend on the input signal level. Figure 14 illustrates the behavior.

The remedy for this problem is very simple. A common-mode inductor is inserted between the twisted pair and the differential receiver, with the output loaded to ground through a specific network, as illustrated in Figure 15. A common mode inductor presents zero inductance to differential signals, but a high inductance to common mode signals. The simple "T" output network presents capacitive loading to common mode signals and no loading to differential mode signals. The result is strong attenuation of common mode noise prior to the differential receiver and virtually no attenuation of differential signal.

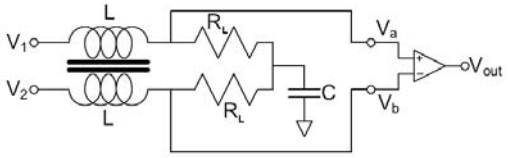

Figure 15: Differential receiver with common mode choke and capacitive loading.

The addition of this common mode attenuator was extremely effective in removing the otherwise very strong switching noise infiltration to the sensor cable. With the addition of the differential receiver, the broadband (unfiltered) received noise level was on the order of 50 mV RMS: improvements to ground management and enclosure shielding in the differential receiver would be expected to realize further improvements.

CONCLUSIONS

Existing finite element models for shielded or unshielded twisted pair cables were extended to permit asymmetric drive and to model skin effects over a broad range of frequencies, suitable for transient simulation. These models were validated individually and shown to provide high fidelity to experimental data, except with regard to coupling from primary conductors to the shield at high frequencies.

The models were then joined capacitively to simulate cross-talk between a coil drive cable and an adjacent sensor cable. The fidelity of this model was relatively poor but judged useful for qualitative assessments.

Based on the modal structure of the cable model, it was determined that even cables as long as 1 km will not be expected to introduce significant dynamic effects in the frequency ranges ordinarily examined in AMB system models. However, capacitive loading by the cables was speculated to potentially produce stability problems for switching power amplifiers and this was discovered experimentally. A corrective action, in the form of small inductors inserted into the drive cable at the power amplifier, was suggested but not investigated.

Finally, methods to reduce noise ingress to sensor signal transmissions from coil drive cables were investigated. It was found that using a properly constructed differential transmit/receive structure in combination with a common mode choke at the receive end was very successful in attenuating this noise.

REFERENCES

[1] Ahmed, S. S., Rajaratnam M., Ahmad H., and Sidik, M. A. B. "Potential Benefits of Using Distributed Parameter Model for Transmission Lines in Power System Analysis," IEEE *Power Engineering Review*, pp. 53-56, October 2002.

[2] Bartnikas, R. *Power and Communication Cable: Theory and Applications*, New York: McGraw-Hill, 2000.

[3] Demarest, K. R. *Engineering Electromagnetics*, New Jersey: Prentice Hall, 1998.

[4] Elder, N. R., "Effects of Extended Cabling on AMB Electrical Systems," M. S. Thesis, University of Virginia, May 2008.

[5] Sadiku, M. N. *Elements of Electromagnetics*, New York: Oxford University Press, 2001.

[6] Spadacini, G., Bellan, D., Pignari, S. A. "Impact of Twist Non-Uniformity on Crosstalk in Twisted-Wire Pairs," IEEE EMC, pp. 483-488, Aug 2003.

[7] Stolle, R. "Electromagnetic Coupling of Twisted Pair Cables," IEEE *Journal on Selected Areas in Communications*, VOL. 20, NO. 5, June 2002.

[8] Wheeler, H. "Formulas for the Skin Effect," Proceedings of the Institute of Radio Engineers, pp. 412-424, September 1942.